

Studying Soil Salinity and Its Relations with Microtopography and Vegetation at Field Scale

Chang-Wei Zhao^{1,2}, Lu Xu^{1,2}, Zhi-Chun Wang^{1*}, Yun-He Wang^{1,2}, Chun-Ming Chi³

¹Northeast Institute of Geography and Agroecology, Chinese Academy of Sciences, Changchun 130012, China

²Graduate University of Chinese Academy of Sciences, Beijing 100049, China

³Tarim University, Alar, Xinjiang 843300, China

Received: 27 December 2012

Accepted: 2 March 2013

Abstract

Spatial variation of soil salinity and sodicity is a typical characteristic of Songnen Plain grasslands in northeast China. Best management practices and grassland productivity improvement require further understanding of the relationships among the causal factors at field scale. A field soil survey for the interactions among salinity, microtopography, and vegetation was conducted on a 2.8 hectare saline sodic grassland at Da'an Sodic Land Experimental Station, Chinese Academy of Sciences, northeast China. Salinity of the soil decreases by depth increment with Na^+ and HCO_3^- as the dominant ions. Soil salinity and sodicity parameters measured include pH, electrical conductivity for 1 to 5 soil-water extracts ($\text{EC}_{1:5}$), apparent electrical conductivity (EC_a), sodium adsorption ratio, and exchangeable sodium percentage. Soil salinity is in an order of slope > mound > depression for microtopography and soil under *S. corniculata* community is in severe salinity, while there is no significant difference under *P. australis*-*A. mongolica* and *P. australis* communities. The water and salt regime in various microtopographical conditions also is discussed.

Keywords: spatial variation, soil salinity and sodicity, microtopography, vegetation community

Introduction

Land degradation induced by negative natural factors or human activities is a very important problem that cannot be neglected in arid or semi-arid regions [1-3]. In northeast China a large area of land is affected by salts as a semi-arid climate, and most of them are natural grasslands that have not been reclaimed for agronomical purposes [4, 5]. Due to long-term deficiency of proper input and management, problems emerged by the end of the last century as the degradation of the grasslands and the recession of the stock breeding, which affected the economic sustainability of region [6-8]. From then on an ambitious

project for restoration of the grassland affected by salts was launched by the local government, and the restriction of grazing and mowing was the major measure that has been technically performed [9]. For more than 10 years of restoring, the grassland has been restored to a degree of part covered by grasses. However, not all the grasslands could be restored to a high productivity attribute to the soil salinization and sodicification. Soil productivity varies seriously with salinity in the field, and the vegetation was instrumentally shaped by various species of grasses, even on a small scale [10, 11].

Spatial variation of soil properties related to salts is possibly caused by soil heterogeneity and variations of external factors, including shallow groundwater, microtopography, seasonal water logging, and human activities [12].

*e-mail: wangzhichun@neigae.ac.cn

It exhibits a subsequence of the vegetation cover heterogeneity; and a causal factor of the heterogeneity of the vegetation pattern on the saline and sodic soil could be considered a complexity of various environmental consequences. The importance of the spatial distribution of soil properties has been mentioned in former research of the Songneng plain [13, 14], but the relationship among the causal factors was not demonstrated by situ investigation of the soil. Soils affected by salts is a continuum that varies in spatial and temporal scales; therefore, the consequences that we can reach now is a main subsequent cause to the future [15, 16].

Better understanding the main cause of the heterogeneity of the soil properties is essential for enhancing grassland productivity [17, 18]. The subject of this article is to analyze the causes of the variation of the salinity and sodicity of the soil by investigating the relationship between salinity and microtopography, water content, and microtopography, and by comparing salinity sodicity under different vegetation communities.

Materials and Methods

Site Description

The study site is a 2.8 ha saline sodic grassland at Da'an Sodic Land Experimental Station, Chinese Academy of Sciences, which is located in west Jilin province, northeast China. The climate of the region could be considered continental semi-arid monsoon, for the annual mean temperature is around 4.7°C, the pan evaporation and precipitation are 1,000-2,500 mm and 370-400 mm, respectively, and rainfall mainly concentrates in July and August [19]. There is a long period of freezing time in a year, from early in November to later May, and the insolation and effective accumulated temperature is sufficient (2,885.5 h and 2,996.2°C a year) for plant growth to balance the long period of low temperature in a year.

Sixteen species of native grasses were investigated in this study site. Among these, just one species of the grasses could be considered a salt-tolerable plant (halophyte, *Suaeda corniculata*) and the other 15 species could be considered glycophyte according to Glenn et al. [20]. Five communities dominated by *Suaeda corniculata* (C. A. Mey.) Bunge, *Puccinellia tenuiflora* (Turcz.) Scribn., *Phragmites australis* (Cav.) Trin. ex Steud. and *Artemisia mongolica* Fisch. et al. Bess., and *Lactuca sibirica* (L.) Benth., were confined, respectively [21], and communities dominated by a particular grass are situated on a particular position on this study site.

The *Suaeda corniculata* community is poor covered xeric grassland located on the middle of the gradual slope. The structure of the community is simple, and just one species of a forb (*S. corniculata*) could develop on this site. The *Puccinellia tenuiflora* community is good covered grassland located on the edges of the depressions around the *P. australis* and *A. mongolica* communities. The community dominated by *S. corniculata* is situated in the upper

position of the slope; a neighbor to this *P. tenuiflora* community, the structure of the community is simple too, as other species of grasses were rarely found in this cereal-dominated grassland. The *Phragmites australis* – *Artemisia mongolica* community is good covered grassland located around the depressions, which are dominated by the two fast-growing grass species. *P. australis* is a tall rhizomatous perennial and *A. mongolica* is a biennial forb. *Phragmites australis* is good covered mesic vegetation located in the depressions. As the rainfall is sufficient in summer, it became waterlogged, and other species of grass could also rarely be found in this community. *Lactuca sibirica* is good covered meso-xeric vegetation located in smaller depressions. The structure of this community is more complicated than the former four.

The grassland has been preserved for several years since 2001, mowing and grazing is prohibited in this field, for the serious degradation of the grassland caused by excessive grazing. For a nearly one-decade restoration of the grassland, this field site was all virtually vegetated and barren.

Field Survey and Soil Sampling

The field work of the situ survey, soil sampling, and investigation of communities were carried out from August to September 2009. Our experiment consisted of:

- (i) surveys of the environmental factors for community level
- (ii) examination of the community structure, biomass, and α biodiversity index.

To examine the environmental factors we employed a dumpy level to map the relative elevations of micro topography, and an electromagnetic (EM) instrument (EM-38) developed by Geonics Ltd., Canada, to map the spatial dis-

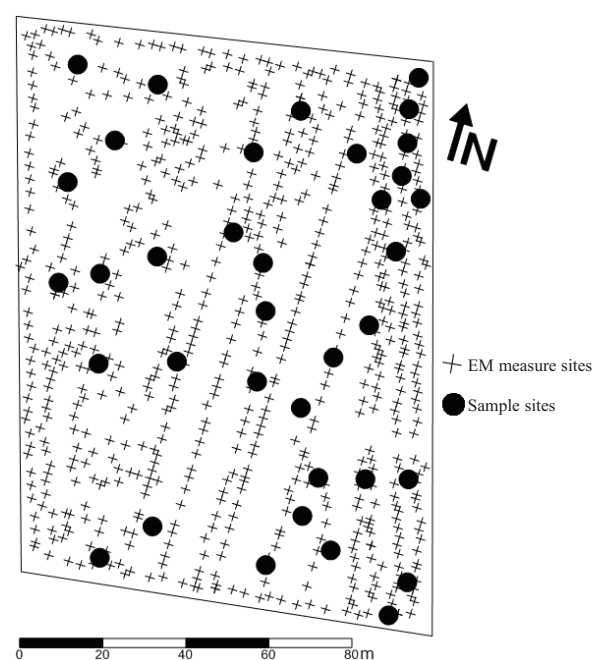


Fig. 1. Map of study site for EM measurement sites and soil sampling and grass quadrat sites.

Table 1. Main statistics for 0-10 cm depth sampled from 36 sites.

Soil property	Mean	SE	Max.	Min.	SD	CV	Skewness
EC _{1:5} (dS/m)	0.8	0.1	2.86	0.14	0.61	76.53	1.93
pH	9.66	0.12	10.47	7.79	0.72	258.73*	-1.26
Na ⁺ (mmol _c /L)	11.38	1.37	37.7	2	8.22	72.22	1.57
Ca ⁺⁺ +Mg ⁺⁺ (mmol _c /L)	2.14	0.34	6.83	0.04	2.02	94.41	0.98
CO ₃ ²⁻ (mmol _c /L)	1.53	0.33	6.88	0	2.01	131.53	1.4
HCO ₃ ⁻ (mmol _c /L)	8.91	1.03	28.2	0.54	6.18	69.39	1.17
Cl ⁻ (mmol _c /L)	1.81	0.27	8.39	0.15	1.63	89.8	2.11
SO ₄ ²⁻ (mmol _c /L)	0.6	0.14	4.31	0.12	0.86	144.17	2.72
CEC (cmol _c /kg)	44.17	3.36	86.5	14.25	20.14	45.61	0.47
Exchangeable sodium (cmol _c /kg)	20.23	1.88	52.8	6.4	11.29	55.82	0.97
ESP (%)	52.86	4.54	97.02	7.4	27.23	51.5	-0.05
SAR ((mmol _c /L) ^{1/2})	15.75	2.34	65.55	3.86	14.05	89.17	2.03

*Calculating with the concentration of hydrogen ion in mol/L.

tribution of salinity with a GPS receiver [22]. Soil properties under particular communities were obtained through core sampling of the profile. We selected 36 sites to measure the apparent electrical conductivity (EC_a) and take the core samples. The core samples were drilled to a depth of 120 cm with a manual auger, with the interval of 10 cm for the upper layer of the soil profile to a depth of 20 cm, and to the deeper with interval of 20 cm to a depth of 120 cm.

Electrical conductivity (EC_{1:5}) was determined by a DDS-307 conductivity meter (Shanghai precision scientific instrument Co., Ltd., China). The pH value of the 1:5 suspension was determined by a LIDA920 (Shanghai LIDA Instrument Factory). The cations Na⁺, K⁺, Ca²⁺, and Mg²⁺ were determined using induced couple-plasma spectroscopy (GBC, scientific equipment Pty Ltd., Australia). The exchangeable cations as Na⁺, K⁺, Ca²⁺, and Mg²⁺ were compulsively exchanged with ammonium acetate in a solution, and were determined using induced couple-plasma spectroscopy. The cation exchange capacity (CEC) was the sum of the cations. The anions determined in this experiment included CO₃²⁻, HCO₃⁻, Cl⁻, and SO₄²⁻. All these anions were determined by Potentiometric titration. The CO₃²⁻ and HCO₃⁻ were titrated with sulphuric acid. The Cl⁻ and SO₄²⁻ were titrated with AgNO₃ and Pb(NO₃)₂, respectively. All the soluble cations and anions were in mmol_c·L⁻¹, while the exchangeable cations and CEC were in cmol_c·kg⁻¹.

The Sodium adsorption ratio (SAR) was calculated with analysis results of the Na⁺, Ca²⁺, and Mg²⁺. In the following equation the values of the ions are equivalent concentrations for calculating the SAR.

$$SAR = \frac{Na}{\sqrt{\frac{Ca + Mg}{2}}}$$

The exchangeable sodium percentage (ESP) is calculated with the exchangeable cations of the soil. ESP is the percentage for the exchangeable sodium of the cation exchange capacity as the follow equation:

$$ESP = \frac{100 \times ExNa^+}{CEC}$$

The water content was measured by weight. All the samples were collected in 3 days and soil samples were oven-dried at 105°C for 6 hours in aluminum boxes.

Analysis of variance (ANOVA) was performed using Microsoft Office Excel 2003. A semivariogram spherical model was used to analyze the spatial autocorrelation of data. To assess possible linear relationships, linear or non-linear regression models were fitted.

Results

Chemical Properties of the Sample Sites

Soil properties of the 36 sites measured by 1:5 suspensions of soil and water are shown in Tables 1-7. We list the main statistics of soil salinity and sodicity parameters at the depth increment of 0-10, 10-20, 20-40, 40-60, 60-80, 80-100, and 100-120 cm. These statistics show the main components of electrolyte in the soil and variations of soil properties by the coefficient of variation (CV). The electrolyte of the 1:5 suspension of the soil in our study site is predominated by Na⁺ and HCO₃⁻. This is the crucial cause for the high pH of the soil. All the properties measured in this study vary except for pH, for its special algorithm. The CV of EC_{1:5} decrease by depth increment associating with the major dominating electrolyte Na⁺ and HCO₃⁻.

Table 2. Main statistics for 10-20 cm depth sampled from 36 sites.

Soil property	Mean	SE	Max.	Min.	SD	CV	Skewness
EC _{1:5} (dS/m)	1.02	0.1	2.82	0.19	0.62	61.05	1.39
pH	9.85	0.1	10.41	7.68	0.58	412.59*	-2.12
Na ⁺ (mmol/L)	14.29	1.37	40.3	2.5	8.24	57.69	1.22
Ca ⁺⁺ +Mg ⁺⁺ (mmol/L)	3.4	0.41	8.28	0.04	2.48	72.87	0.33
CO ₃ ⁻⁻ (mmol/L)	2.54	0.35	7.07	0	2.11	83.05	0.48
HCO ₃ ⁻ (mmol/L)	11.77	1.11	35.96	2.01	6.69	56.79	1.33
Cl ⁻ (mmol/L)	2.19	0.33	8.35	0.1	1.97	89.82	1.86
SO ₄ ⁻⁻ (mmol/L)	0.53	0.14	4.8	0.11	0.84	160.65	4.01
CEC (cmol/kg)	46.64	2.68	90	21.25	16.06	34.43	0.96
Exchangeable sodium (cmol/kg)	26.26	1.91	58.6	8.6	11.43	43.54	0.82
ESP (%)	60.75	4.03	96.4	9.56	24.2	39.84	-0.39
SAR ((mmol/L) ^{1/2})	22.93	6.83	219.36	3.32	40.95	178.64	3.8

*Calculating with the concentration of hydrogen ion in mol/L.

Table 3. Main statistics for 20-40 cm depth sampled from 36 sites.

Soil property	Mean	SE	Max.	Min.	SD	CV	Skewness
EC _{1:5} (dS/m)	1.02	0.08	2.39	0.31	0.5	48.91	0.98
pH	9.96	0.07	10.51	8.55	0.44	210.36*	-1.35
Na ⁺ (mmol/L)	14.24	1.09	30.2	4	6.54	45.94	0.69
Ca ⁺⁺ +Mg ⁺⁺ (mmol/L)	2.87	0.39	9.66	0.04	2.34	81.56	0.81
CO ₃ ⁻⁻ (mmol/L)	2.53	0.34	7.22	0	2.04	80.92	0.71
HCO ₃ ⁻ (mmol/L)	11.67	1.15	35.47	2.54	6.9	59.1	1.78
Cl ⁻ (mmol/L)	2.33	0.4	10.48	0.08	2.41	103.34	2.08
SO ₄ ⁻⁻ (mmol/L)	0.58	0.15	3.95	0.13	0.88	151.23	3.14
CEC (cmol/kg)	45.99	2.49	84.25	17.75	14.96	32.53	0.13
Exchangeable sodium (cmol/kg)	25.8	2.21	69.4	7.2	13.28	51.46	1.46
ESP (%)	59.39	4.18	96.2	16.18	25.08	42.22	-0.23
SAR ((mmol/L) ^{1/2})	23.65	5.72	166.42	5.08	34.35	145.27	3.11

*Calculating with the concentration of hydrogen ion in mol/L.

To further describe the spatial variation of soil salinity, a semivariogram for each data set was developed for twelve salinity parameters. Results from Table 8 show that nugget/sill ratio values of seven salinity parameters were less than 25%, which indicated a strong spatial autocorrelation for seven salinity parameters, except for five parameters (CO₃⁻⁻, SO₄⁻⁻, CEC, exchangeable sodium, and ESP). The results demonstrated that the spatial variations of seven soil salinity parameters were mainly affected by structural factors, which might include topography, hydrological, and

climatic condition. The other five parameters were mainly affected by random factors.

Correlation between EC_a and EC_{1:5}

The correlation between EC_a and EC_{1:5} is significant ($P < 0.0001$), which indicates that the spatial distribution of EC_{1:5} expressed by EC_a could be considered reliable. The EM_H and EM_V in the equations by simple linear regression represent the EC_a values that measured by the EM38 in the

Table 4. Main statistics for 40-60 cm depth sampled from 36 sites.

Soil property	Mean	SE	Max.	Min.	SD	CV	Skewness
EC _{1:5} (dS/m)	1.03	0.08	2.31	0.3	0.46	44.85	1.17
pH	9.93	0.07	10.41	9.01	0.4	124.31*	-1.02
Na ⁺ (mmol _c /L)	14.27	1	30.9	4.3	6.01	42.14	0.83
Ca ⁺⁺ +Mg ⁺⁺ (mmol _c /L)	2.44	0.33	6.46	0.03	1.98	81.43	0.51
CO ₃ ⁻⁻ (mmol _c /L)	2.66	0.42	9.15	0	2.5	93.95	1.08
HCO ₃ ⁻ (mmol _c /L)	11.92	0.99	27.36	3.66	5.95	49.88	1.08
Cl ⁻ (mmol _c /L)	2.37	0.36	9.29	0.14	2.18	91.93	1.72
SO ₄ ⁻⁻ (mmol _c /L)	0.66	0.12	3.65	0.04	0.73	110.79	2.34
CEC (cmol _c /kg)	41.57	2.68	78.5	16.25	15.87	0.38	0.81
Exchangeable sodium (cmol _c /kg)	22.5	1.74	54.4	8.8	10.27	45.63	1.29
ESP (%)	57.94	4.02	97.39	18.11	23.44	40.45	0.03
SAR ((mmol _c /L) ^{1/2})	27.93	6.8	198.47	6.18	40.8	146.08	2.99

*Calculating with the concentration of hydrogen ion in mol/L.

Table 5. Main statistics for 60-80 cm depth sampled from 36 sites.

Soil property	Mean	SE	Max.	Min.	SD	CV	Skewness
EC _{1:5} (dS/m)	0.84	0.06	1.85	0.33	0.36	42.82	0.96
pH	9.91	0.07	10.39	8.88	0.42	138.11*	-0.95
Na ⁺ (mmol _c /L)	11.58	0.77	23.5	4.7	4.62	39.94	0.71
Ca ⁺⁺ +Mg ⁺⁺ (mmol _c /L)	3.39	0.49	10.04	0.04	2.93	86.49	0.87
CO ₃ ⁻⁻ (mmol _c /L)	2.06	0.35	7.67	0	2.09	101.15	1.16
HCO ₃ ⁻ (mmol _c /L)	9.87	0.9	24.42	2.06	5.43	54.95	0.66
Cl ⁻ (mmol _c /L)	2.24	0.34	11.28	0.13	2.06	92.3	2.66
SO ₄ ⁻⁻ (mmol _c /L)	0.64	0.19	4.74	0.13	1.14	177.07	2.7
CEC (cmol _c /kg)	38.56	2.42	76.75	19.5	14.51	37.63	0.92
Exchangeable sodium (cmol _c /kg)	21.29	1.8	48.4	6.2	10.78	50.62	0.95
ESP (%)	58.47	4.14	96	14.96	24.81	42.44	-0.19
SAR ((mmol _c /L) ^{1/2})	16.43	4.21	143.24	3.21	25.26	153.73	4.34

*Calculating with the concentration of hydrogen ion in mol/L.

horizontal and the vertical configuration, respectively. The r-square values indicate the strength of association between EC_{1:5} and the EC_a. We chose the best-fitting equation (Eq. 1 and Eq. 2) to express the spatial distribution of EC_{1:5} for the upper layer of the depths to 0-10 cm and 10-20 cm where the roots mainly spread.

$$0-10 \text{ cm: } EC_{1:5} = 1.09 EM_H - 0.23 \quad (1)$$

(r² = 0.52 P < 0.0001)

$$10-20 \text{ cm: } EC_{1:5} = 1.27 EM_H - 0.21 \quad (2)$$

(r² = 0.69 P < 0.0001)

$$0-10 \text{ cm: } EC_{1:5} = 1.05 EM_V - 0.41 \quad (3)$$

(r² = 0.42 P < 0.0001)

$$10-20 \text{ cm: } EC_{1:5} = 1.24 EM_V - 0.32 \quad (4)$$

(r² = 0.58 P < 0.0001)

Relationship between Micro-Topography and Salinity

Soil EC_a and EC_{1:5} of 0-20cm layers varied with the surface microtopography (Fig. 2). The relative relief ranges from 0-42 cm in this study site, and the slopes are very gradual.

Table 6. Main statistics for 80-100 cm depth sampled from 36 sites.

Soil property	Mean	SE	Max.	Min.	SD	CV	Skewness
EC _{1:5} (dS/m)	0.72	0.05	1.45	0.32	0.29	40.46	0.89
pH	9.86	0.07	10.4	9	0.4	111.73*	-0.68
Na ⁺ (mmol _c /L)	9.99	0.66	17.9	4.5	3.94	39.42	0.7
Ca ⁺⁺ +Mg ⁺⁺ (mmol _c /L)	2.33	0.32	9.37	0.04	1.9	81.53	1.72
CO ₃ ⁻⁻ (mmol _c /L)	1.46	0.27	6.77	0	1.63	111.91	1.72
HCO ₃ ⁻ (mmol _c /L)	7.67	0.64	17.62	0.95	3.83	49.93	0.72
Cl ⁻ (mmol _c /L)	2.02	0.29	8.63	0.31	1.74	85.82	2.2
SO ₄ ⁻⁻ (mmol _c /L)	0.79	0.23	6.81	0.13	1.35	171.68	3.29
CEC (cmol _c /kg)	33.26	2.24	67	18.75	13.46	40.48	0.8
Exchangeable sodium (cmol _c /kg)	19.36	1.88	48.6	6	11.28	58.24	1.02
ESP (%)	59.82	4.13	96.41	12.18	24.81	41.47	-0.33
SAR ((mmol _c /L) ^{1/2})	13.08	2.55	98.01	4.88	15.29	116.9	5.18

*Calculating with the concentration of hydrogen ion in mol/L.

Table 7. Main statistics for 100-120 cm depth sampled from 36 sites.

Soil property	Mean	SE	Max.	Min.	SD	CV	Skewness
EC _{1:5} (dS/m)	0.62	0.05	1.41	0.25	0.27	44.06	1.17
pH	9.79	0.07	10.34	8.83	0.44	127.91*	-0.75
Na ⁺ (mmol _c /L)	8.5	0.62	20.2	3.5	3.7	43.58	1.23
Ca ⁺⁺ +Mg ⁺⁺ (mmol _c /L)	2.09	0.36	8.57	0.04	2.17	103.76	1.76
CO ₃ ⁻⁻ (mmol _c /L)	1.58	0.32	7.16	0	1.91	120.4	1.79
HCO ₃ ⁻ (mmol _c /L)	6.74	0.62	15.2	1.39	3.7	54.88	0.59
Cl ⁻ (mmol _c /L)	1.99	0.36	8.88	0.22	2.18	109.37	2.33
SO ₄ ⁻⁻ (mmol _c /L)	0.52	0.11	2.92	0.13	0.65	123.66	2.2
CEC (cmol _c /kg)	34.99	2.54	72.75	14	15.23	43.53	0.7
Exchangeable sodium (cmol _c /kg)	17.58	1.72	47.2	3.6	10.33	58.77	1.14
ESP (%)	52.77	3.95	94.05	11.34	23.71	44.93	-0.02
SAR ((mmol _c /L) ^{1/2})	13.72	2.65	93.29	3.97	15.9	115.9	4.03

*Calculating with the concentration of hydrogen ion in mol/L.

The highest salinity was spotted on the slopes while the lightest was situated in the depressions. The salinity on the mound was higher than the depressions but much lighter than the slope. The highest value of the coefficient of variation for EC_{1:5} was in the depressions, indicating that the spatial distribution of salinity was more complex than that in the slop and mound of the micro-topography. Indeed, the range of EC_{1:5} values were from 0.1 to 0.86 of the depth of 0-10 cm and 0.11 to 0.97 of the 10-20 cm (Table 9), which means that soils in lower places could be characterized to be saline or nonsaline referring to the former

reports [17]. However, there was no clear border between these two layers of soil in sight of the depressions within this field.

Relationship between Water Content and Micro-Topography

By comparing the mean values of water contents of the three features of micro-topography we found the highest water content of the upper layer of the soil was in the depressions (Table 10), and it decreased with the micro-

Table 8. Summary of best-fit models for salinity parameters in 0-10 cm soil layer (n=36).

Parameter	Best-fit model	Nugget, C_0	Sill, C_0+C	Range (m), A_0	C_0/C_0+C (%)	R^2	RSS
$EC_{1.5}$ (dS/m)	Spherical	0.0001	0.1012	44.7	0.001	0.881	1.185E-03
pH	Spherical	1.000E-005	5.360E-003	29.9	0.002	0.635	9.375E-06
Na^+ (mmol _c /L)	Spherical	0.001	0.453	39	0.002	0.799	0.040
$Ca^{++}+Mg^{++}$ (mmol _c /L)	Spherical	0.001	0.373	27.3	0.003	0.588	0.048
HCO_3^- (mmol _c /L)	Spherical	0.001	0.469	35.3	0.002	0.618	0.102
Cl^- (mmol _c /L)	Spherical	0.0001	0.276	49.6	0.001	0.909	6.093E-03
SAR ((mmol _c /L) ^{1/2})	Spherical	0.105	0.660	105.2	0.249	0.775	0.065

relieve within this study site. With the increment of the depths of different features of the micro-topographies, the driest place could be confined on the top of the mounds. However, there were no significant differences between the water contents on the gradual slopes and the depressions in the deeper layers of the profiles. The water contents

increased with the increment of the depths of these three features of the micro-topographies, but there were no significant differences among the downward layers under 20 cm of the mound sites. The maximum value of the water content of the slopes was spotted at a depth of 80-100 cm, and the maximum value for the depressions was found at

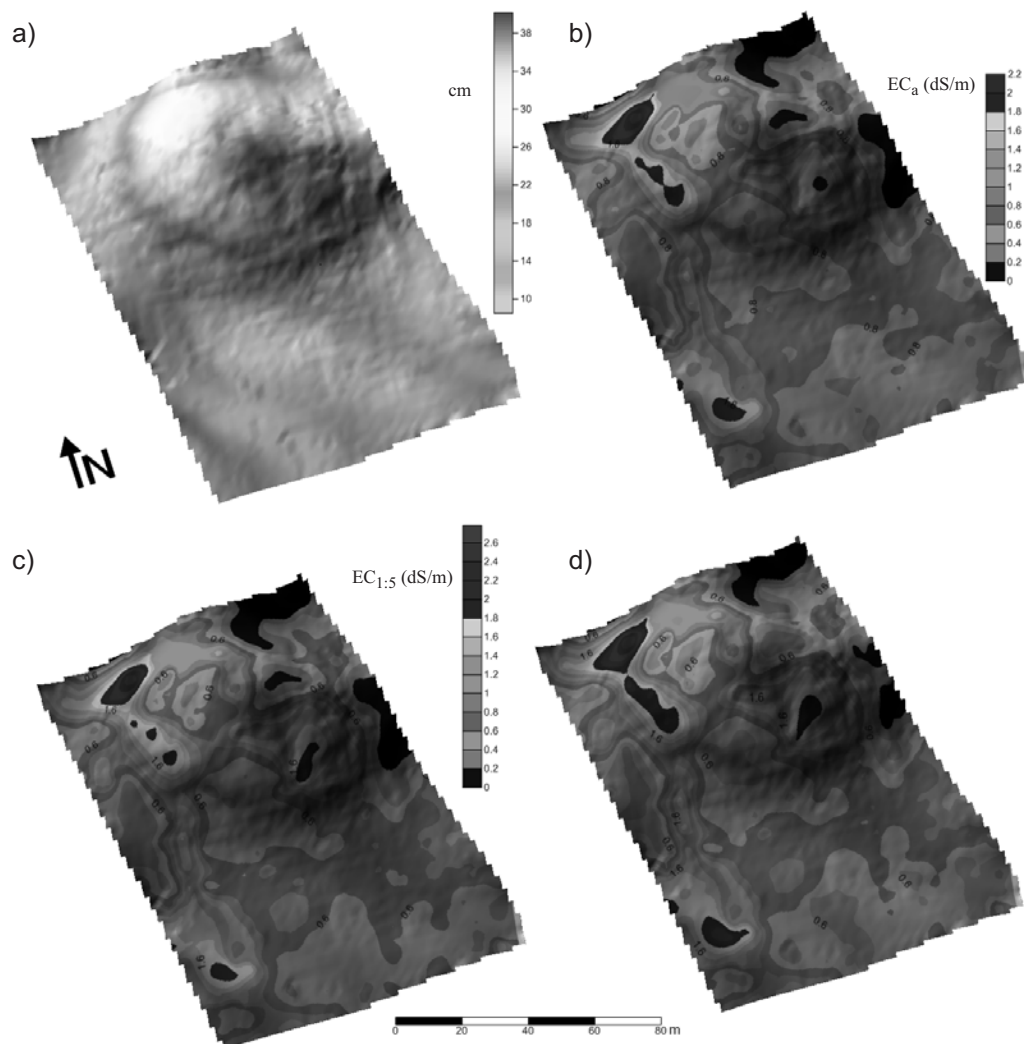


Fig. 2. 3D surface map of micro-relief (a) overlapped by the contour colored map of the apparent soil electrical conductivity (EC_a). We choose the EC_a measured in horizontal configuration here (b), the electrical conductivity of 1:5 suspensions ($EC_{1.5}$) of depth of 0-10 cm (c), and the electrical conductivity of 1:5 suspensions ($EC_{1.5}$) of depth of 10-20 cm (d).

Table 9. Electrical conductivity ($\text{dS}\cdot\text{m}^{-1}$) of 1:5 suspension ($\text{EC}_{1:5}$) of the soil from upper layers of distinguishing features of the micro-topography.

	Mean	SE	SD	CV (%)	Skewness	Min.	Max.
0-10 cm							
Mound	0.68	0.05	0.23	33.82	-0.55	0.15	1.05
Gradual slope	1.3	0.11	0.58	44.62	0.31	0.54	2.86
Depression	0.51	0.04	0.24	47.06	-0.47	0.1	0.86
10-20 cm							
Mound	0.88	0.08	0.29	32.95	0.33	0.42	1.41
Gradual slope	1.73	0.14	0.58	33.53	-0.08	0.84	2.82
Depression	0.55	0.04	0.23	41.82	-0.46	0.11	0.97

Table 10. Mass water content (%) of the soil sampled from upper layers of distinguishing features of the micro-topography.

	Mean	SE	SD	CV (%)	Skewness	Min.	Max.
0-10 cm							
Mound	7.38	1.08	3.06	41.54	0.82	4.06	12.65
Gradual slope	8.56	0.74	3.20	37.41	0.64	2.22	16.34
Depression	11.42	1.26	5.18	45.39	1.09	4.06	24.89
10-20 cm							
Mound	12.49	0.89	2.52	20.18	-0.40	8.51	15.38
Gradual slope	13.59	0.56	2.43	17.88	-0.27	8.23	17.15
Depression	16.58	1.36	5.62	33.89	1.13	8.51	31.62
20-40 cm							
Mound	12.46	0.89	2.52	20.23	-0.92	7.60	15.58
Gradual slope	15.53	0.53	2.31	14.84	0.33	11.67	20.37
Depression	15.71	1.01	4.17	26.56	0.30	7.60	24.92
40-60 cm							
Mound	12.88	1.08	3.04	23.62	-1.03	6.94	16.99
Gradual slope	14.75	0.44	1.92	13.01	0.49	11.46	18.65
Depression	15.82	0.87	3.58	22.65	-1.05	6.94	20.08
60-80 cm							
Mound	12.74	0.82	2.33	18.31	-1.97	7.49	14.57
Gradual slope	15.35	0.59	2.59	16.87	0.24	10.49	20.89
Depression	16.02	1.07	4.40	27.50	0.85	7.49	27.90
80-100 cm							
Mound	13.43	0.47	1.33	9.88	-0.50	11.25	15.15
Gradual slope	18.13	1.51	6.57	36.23	1.61	11.59	34.68
Depression	15.75	0.67	2.76	17.54	0.31	11.25	20.84
100-120 cm							
Mound	14.75	0.49	1.39	9.39	0.51	13.35	16.53
Gradual slope	15.81	0.69	3.02	19.11	0.66	11.44	22.29
Depression	17.68	1.21	5.00	28.30	2.59	13.35	34.44

100-120 cm, which was the deepest layer that we sampled. The CV values indicate the spatial variation of the soil-water content. The minimum value of the CV was on the slopes, and CV of the depressions was higher than the other two features of the micro-topographies for the same depths from the surface. The CV decreased by increment of the depth, and the maximum was in the upper layers of 0-20 cm.

More water gathered in the depressions and it became waterlogged in the rainy season from June to early August. Due to poor infiltration, the rain water could not sufficiently permeate the surface of the soil on the slope and the mound sites; at the same time, the severe evaporation of the pan water of this area, the soil moisture of the upper layers was very low on the slopes and mound sites compared with the depressions. The variation in micro-topography results in a serious heterogeneity of the water content within this field scale (all the CV values of upper layer were more than 35 percent), especially in the depressions attributed to the different size of these small catchments.

In this study site, three small catchment areas were spotted. The larger one was waterlogged in the whole season of rainfall, from June to early August, and continuous ponding condition did not terminate until the ponding water evaporated in September. For the other two smaller catchment areas, less water gathered and the soil would be dried immediately after the rain season.

Soil Salinity and Sodicity Properties under Particular Communities

Soil salinity and sodicity properties under various grass communities are given in Fig. 3. There are significant differences in $EC_{1:5}$ of the profiles among the five communities ($F_{4,32} = 14.586, P < 0.001$). The *S. corniculata* community was the most severe in salinity, and the *L. sibirica* community was the lightest. There was no significant difference between *P. australis*-*A. mongolica* and *P. australis* communities in $EC_{1:5}$ ($F_{1,10} = 0.39, P = 0.54$). Salt accumulation could be found in the subsoil layers of the profile under all five types of vegetation. Even for the poor covered vegetation of *S. corniculata* community, the average value of $EC_{1:5}$ of 10-20 cm depth was higher than upper layer of 0-10 cm depth ($F_{1,14} = 0.465, P = 0.507$): not significant, but a leaching process could be considered somehow. A similar process also could be found in the profiles under the other four communities (Fig. 1 a). There are significant differences in pH values of the profiles among the five communities ($F_{4,32} = 19.3794, P < 0.001$), and all the pH values were high due to the high values of the ESP and the predominant component of the anions of HCO_3^- in the soil suspensions (Tables 1-7). Thus, the sodicification can be considered for soils under all five communities. This is the major cause of the harsh physical conditions for the rhizosphere, which results in poor hydraulic conductivity for the soil water. Less water moves downward into the sublayers of

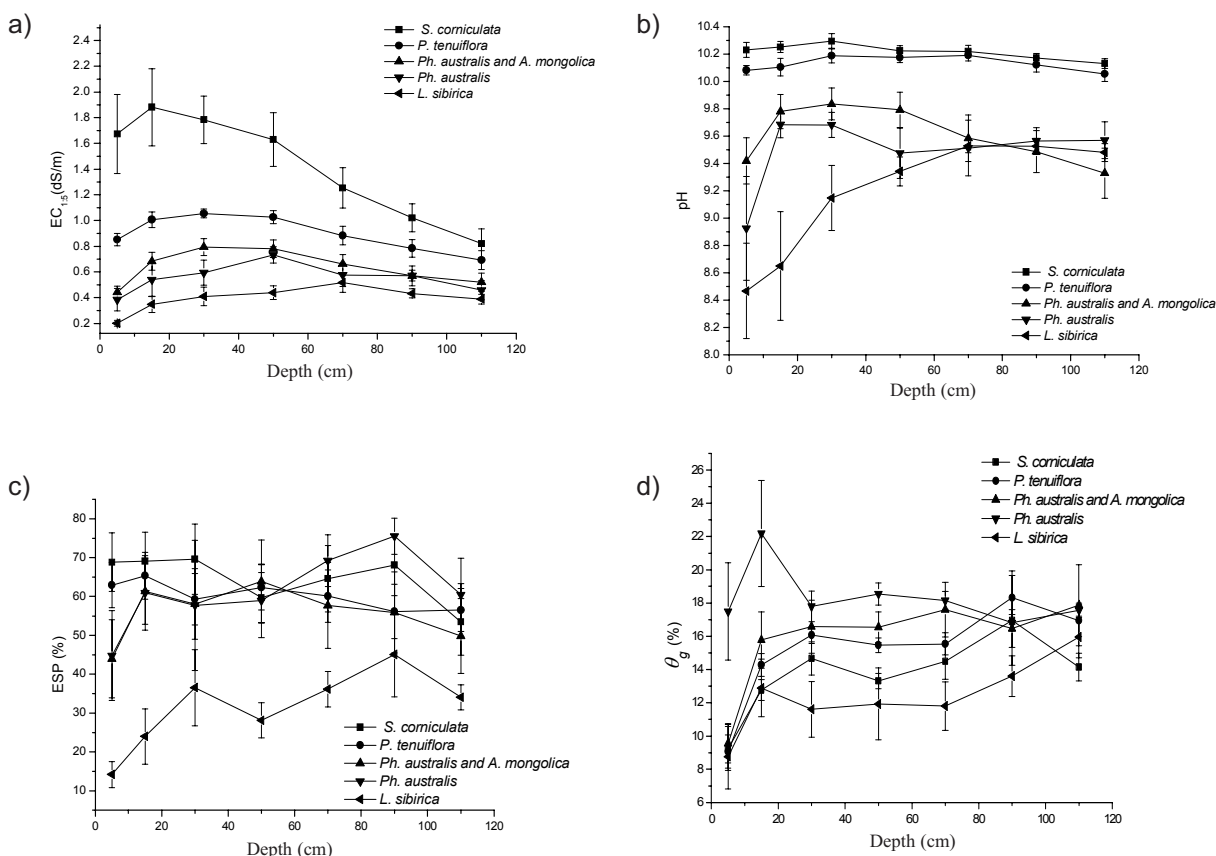


Fig. 3. Select soil properties under particular communities.

the profiles, therefore the water content of the soil profile varies in vertical direction, significantly. The water content is mostly affected by the precipitation and evaporation in the upper layers that the roots spread. There were no significant differences in the deeper layers for water content among these five vegetation situations. Both the *P. australis* and *L. sibirica* communities situated in the depressions: however, *P. australis* could dominate the ponding position well while *L. sibirica* could not be found in this waterlogged condition. The depressions dominated by *P. australis* gathered more water and waterlogged in summer. Water ponding on the surface of the soil would be exceeding saturation because of the poor infiltration rate of the subsoil. As a result, the water content of this position is higher than the other four vegetation-covered positions in dry autumn.

Discussion

The continuous variation of the salinity could induce the abrupt alteration of the vegetation types. In this experiment, the range of salinity varied from the slope to the depressions continuously. The salinity of the upper layers decreased from the higher positions to the depressions gradually, and the most accumulation of salts for the upper layers was under the vegetation of *S. corniculata*, which is the higher position of the slope. The vegetation of *P. tenuiflora* also situated on the slope, but lower than the *S. corniculata* in position. There is a clear boundary between the two, and the salinity of the root zone soil of these two communities was significantly different.

Similar conclusions were common in the salt marshes, caused by the tide rhythm and the distance between the locations of the communities and seashore reported by the former studies [23]. While for the inland grassland like where we conducted this investigation, precipitation is the major water resource, and rainwater could be considered the main driving force to the movement of the salts in the upper layers. Due to the high percentage of exchangeable sodium, the soil structure is severely unstable, resulting in a very low final infiltration rate [24]. Once the surface of the soil was crashed by the raindrops, the soils dispersed and clay particles and sands were detached, then the poor pores were sealed immediately. Therefore the water cannot go any further into the profiles of the soil, and resulted in water runoff.

Even in summer rainfall is sufficient; the salts in the upper layer of slopes could not receive a good leaching. There is much runoff water running into the depressions, bringing the salts from the surface of the slopes. The salts accumulated in the upper layer of the soil. In this study, severe variation of the salinity did not result in an alteration of the vegetation. Soil in smaller depressions is in favorable physical and chemical condition and rich biodiversity.

Conclusions

The variation of soil salinity and sodicity and its relationship with land microtopography and vegetation were

investigated in situ in west Jilin province, northeast China. Salinity of the soil decreases by depth increment with Na^+ as the dominant cation and HCO_3^- and the dominant anion. With the correlation of EC_a and $\text{EC}_{1:5}$, EC_a were used to characterize the spatial distribution of soil salinity. Soil salinity is in an order of slope > mound > depression. The highest water content of the upper layer of the soil was in the depressions, and it decreased with the increment of micro-relieve. However, the water contents were not significantly different between the gradual slopes and the depressions for the deeper layers of the profiles. Soil salinity and sodicity properties vary with grass communities. Severe salinity is found under the *S. corniculata* community, while there is no significant difference under *P. australis* – *A. mongolica* and the *P. australis* communities.

Acknowledgements

This study was supported by the Chinese Academy of Sciences Action Plan for the Development of Western China (KZCX3-XB3-16), the Nonprofit Industry Financial Program of the Ministry of Agriculture of China (200903001-06), and the National Natural Science Foundation of China (41071022).

References

1. BAI Z.G., DENT D. Recent Land Degradation and Improvement in China. *Ambio*. **38**, 150, **2009**.
2. ALADOS C.L., PUIGDEFABREGAS J., MARTINEZ-FERNANDEZ J. Ecological and socio-economical thresholds of land and plant-community degradation in semi-arid Mediterranean areas of southeastern Spain. *J. Arid Environ.* **75**, 1368, **2011**.
3. ZUO X.A., ZHAO H.L., ZHAO X.Y., GUO Y.R., YUN J.Y., WANG S.K., MIYASAKA T. Vegetation pattern variation, soil degradation and their relationship along a grassland desertification gradient in Horqin Sandy Land, northern China. *Environ. Geol.* **58**, 1227, **2009**.
4. GAO Y.J., XI J. Coordinate Developing of Economy and Ecology Protection in Songnen Plain Reservior. *Environment Materials and Environment Management Pts 1-3* **109**, 113, **2010**.
5. WANG Z.M., SONG K.S., ZHANG B., LIU D.W., REN C.Y., LUO L., YANG T., HUANG N., HU L.J., YANG H.J., LIU Z.M. Shrinkage and fragmentation of grasslands in the West Songnen Plain, China. *Agr. Ecosyst. Environ.* **129**, 315, **2009**.
6. ZHENG S.F., SUN Y. The Analysis of Human Factors on Grassland Productivity in Western Songnen Plain. *Procedia Environmental Sciences* **10**, 1302, **2011**.
7. WANG Z.C., LI Q.S., LI X.J., SONG C.C., ZHANG G.X. Sustainable Agriculture Development in Saline-Alkali Soil Area of Songnen Plain, Northeast China. *Chinese Geographical Science* **13**, 171, **2003**.
8. WANG Z.M., SONG K.S., ZHANG B., LIU D.W., REN C.Y., LUO L., YANG T., HUANG N., HU L., YANG H.J., LIU Z. Shrinkage and fragmentation of grasslands in the West Songnen Plain, China. *Agr. Ecosyst. Environ.* **129**, 315, **2009**.

9. YU H.L. Analysis and strategic measures on the drought problems in Songnen Plain. *Water-Saving Agriculture and Sustainable Use of Water and Land Resources* **1**, 817, **2004**.
10. WANG L., SEKI K., MIYAZAKI T. ISHIHAMA Y. The causes of soil alkalization in the Songnen Plain of Northeast China. *Paddy and Water Environment* **7**, 259, **2009**.
11. JIANG S.C., HE N.P., WU L., ZHOU D.W. Vegetation restoration of secondary bare saline-alkali patches in the Songnen plain, China. *Applied Vegetation Science* **13**, 47, **2010**.
12. YANG F. ZHANG G.X. YIN X.R. LIU Z.J. Field scale spatial variation of saline-sodic soil and its relation with environmental factors in West Songnen Plain of China. *International Journal of Environmental Research and Public Health* **8**, 374, **2011**.
13. YANG F., ZHANG G.X., YIN X.R., LIU Z.J. Field-Scale Spatial Variation of Saline-Sodic Soil and Its Relation with Environmental Factors in Western Songnen Plain of China. *International Journal of Environmental Research and Public Health* **8**, 374, **2011**.
14. LIU Q., CUI B.S., YANG Z.F. Dynamics of the soil water and solute in the sodic saline soil in the Songnen Plain, China. *Environmental Earth Sciences* **59**, 837, **2009**.
15. LETEY J., HOFFMAN G.J., HOPMANS J.W., GRATTAN S.R., SUAREZ D., CORWIN D.L., OSTER J.D., WU L. AMRHEIN C. Evaluation of soil salinity leaching requirement guidelines. *Agr. Water Manage.* **98**, 502, **2011**.
16. OSTER J.D., SHAINBERG I. Soil responses to sodicity and salinity: challenges and opportunities. *Aust. J. Soil Res.* **39**, 1219, **2001**.
17. CASTRIGNANO' A., BUTTAFUOCO G., PUDDU R. Multi-scale assessment of the risk of soil salinization in an area of south-eastern Sardinia (Italy). *Precision Agric.* **9**, 17, **2008**.
18. INAKWU O. A., ODEH A. O. Spatial Analysis of Soil Salinity and Soil Structural Stability in a Semiarid Region of New South Wales, Australia. *Environ. Manage.* **42**, 265, **2008**.
19. LIU S.H., KANGY.H., WAN S.Q., WANG Z.C., LIANG Z.W., SUN X.J. Water and salt regulation and its effects on *Leymus chinensis* growth under drip irrigation in saline-sodic soils of the Songnen Plain. *Agr. Water Manage.* **98**, 1469, **2011**.
20. GLENN E.P., BROWN J.J. BLUMWALD E. Salt tolerance and crop potential of halophytes. *Crit. Rev. Plant Sci.* **18**, 227, **1999**.
21. CHI C.M., WANG Z.C. Characterizing Salt-Affected Soils of Songnen Plain Using Saturated Paste and 1:5 Soil-to-Water Extraction Methods. *Arid Land Research and Management* **24**, 1, **2010**.
22. HOSSAIN M.B., LAMB D.W., LOCKWOOD P.V., FRAZIER P. EM38 for volumetric soil water content estimation in the root-zone of deep vertosol soils. *Computer. Electron. Agr.* **74**, 100, **2010**.
23. MOFFETT K.B., ROBINSON D.A., GORELICK S.M. Relationship of Salt Marsh Vegetation Zonation to Spatial Patterns in Soil Moisture, Salinity, and Topography. *Ecosystems* **13**, 1287, **2010**.
24. CHI C.M., ZHAO C.W., SUN X.J., WANG Z.C. Estimating Exchangeable Sodium Percentage from Sodium Adsorption Ratio of Salt-Affected Soil in the Songnen Plain of Northeast China. *Pedosphere.* **21**, 271, **2011**.

